



## Single and multiple drones detection and identification using RF based deep learning algorithm

Boban Sazdić-Jotić<sup>a,\*</sup>, Ivan Pokrajac<sup>b</sup>, Jovan Bajčetić<sup>a</sup>, Boban Bondžulić<sup>a</sup>, Danilo Obradović<sup>a</sup>

<sup>a</sup> Military Academy, University of Defence in Belgrade, Veljka Lukića Kurjaka 33, Belgrade, Serbia

<sup>b</sup> Military Technical Institute, Ratka Resanovića 1, Belgrade, Serbia



### ARTICLE INFO

**Keywords:**

Anti-drone system  
Classification  
Deep learning algorithms  
Detection  
Drone  
Multiple drones

### ABSTRACT

Unmanned aerial systems, especially drones have gone through remarkable improvement and expansion in recent years. Drones have been widely utilized in many applications and scenarios, due to their low price and ease of use. However, in some applications drones can pose a malicious threat. To diminish risks to public security and personal privacy, it is necessary to deploy an effective and affordable anti-drone system in sensitive areas to detect, localize, identify, and defend against intruding malicious drones. This research article presents a new publicly available radio frequency drone dataset and investigates detection and identification methodologies to detect single or multiple drones and identify a single detected drone's type. Moreover, special attention in this paper has been underlined to examine the possibility of using deep learning algorithms, particularly fully connected deep neural networks as an anti-drone solution within two different radio frequency bands. We proposed a supervised deep learning algorithm with fully-connected deep neural network models that use raw drone signals rather than features. Regarding the research results, the proposed algorithm shows a lot of potentials. The probability of detecting a single drone is 99.8%, and the probability of type identification is 96.1%. Moreover, the results of multiple drones detection demonstrate an average accuracy of 97.3%. There have not been such comprehensive publications, to this time, in the open literature that have presented and enlightened the problem of multiple drones detection in the radio frequency domain.

### 1. Introduction

As a fast-developing research area with various improvements, several terms are currently used in literature to entitle unmanned aerial systems (UAS). It is essential to comprehend the difference between confusing terms to understand complex UAS usage in many areas. The term UAS is generally used to describe the entire operating equipment including the aircraft, the ground control station from where the aircraft is operated, and the wireless data link (Hassanalian & Abdelkefi, 2017; Mitka & Mouroutsos, 2017; Yaacoub et al., 2020).

In addition to that, most of the researchers use the term "drone" in everyday language (slang) and research works (jargon), instead of any other official term. Sometimes, both terms are correspondingly used, drone for autonomous aircraft and UAS for the complete system. It is important to highlight that there is an enormous usage growth of UAS in many applications which arises an additional need to regulate air traffic. However, it is unrealistic to expect that every drone pilot (operator) will comply with the air traffic regulations, especially those that have

malicious intentions. Therefore, it is of great importance to have an effective anti-drone (ADRO) system in security-sensitive areas that demand timely detection, identification, localization, and protection from the unauthorized intrusion of drones. To accomplish such a challenging task, it is necessary to engage complex and various types of sensors. These sensors are combined to do the very difficult task of finding and locating aerial targets (drones are small, very agile, and they can operate at relatively low altitudes) in a complex environment (especially in urban areas). The use of these sensors requires the synergy of different technologies, i.e. fusion of radar, audio, video, and/or radio frequency surveillance technologies.

For the purpose of this paper, a new radio frequency (RF) dataset was created and provided in (Sazdić-Jotić et al., 2020). This dataset contains radio signals of various drones working under different flight modes. To this end, three experiments were conducted to record the RF signals of several drones in different scenarios (including the occurrences where several drones operate simultaneously). Afterward, such a RF drone dataset was used to test the ADRO system for drone detection and

\* Corresponding author.

E-mail addresses: [boban.sazdic.jotic@vs.rs](mailto:boban.sazdic.jotic@vs.rs) (B. Sazdić-Jotić), [ivan.pokrajac@vs.rs](mailto:ivan.pokrajac@vs.rs) (I. Pokrajac), [danilo.obradovic@vs.rs](mailto:danilo.obradovic@vs.rs) (D. Obradović).

identification based on deep neural networks (DNN) which are used in (Al-Sa'd et al., 2019). Furthermore, the ADRO system for multiple drones detection was created and its recognition accuracy was verified on this RF drone dataset.

One of the main challenges was to create an appropriate algorithm for multiple drones detection. Moreover, it was imperative to label training data accurately and adjust training parameters for the best results. The key advantage of the proposed algorithm is a high accuracy, regardless of using a non-complex technique (Short-Time Fourier transform, STFT) for preprocessing RF signals. In this manner, the proposed algorithm performs better than other prominent deep learning (DL) algorithms because, after STFT calculation, the data is ready for the training process, without any additional operations. The most critical phase of the proposed algorithm is the preparation of the training data because it is time-consuming. Although we have obtained better results than the authors in (Al-Sa'd et al., 2019), there is still a need to increase the recognition rate of the flight modes of drones that are made by the same manufacturer.

The rest of the paper is organized as follows: section 2 is an overview of the related works in the area of ADRO studies, section 3 describes the system model of the proposed algorithm and the experiments based on it, in section 4 the results and discussions are presented, and finally, the conclusion and future works are given in section 5.

## 2. Related works

In this section, recent RF based ADRO approaches used for detection and identification of intruding drones are reviewed. Moreover, the state-of-the-art DL algorithms are introduced and their implementation in ADRO systems is considered.

### 2.1. Radio frequency drone detection

RF drone detection is specific in several ways compared to other drone detection methods. First of all, radar, audio, and optoelectronic sensors (OES) detect and collect well-known features just from a drone (an autonomous aircraft), while RF sensors perform monitoring of the UAS's radio communication links prearranged between the two participants: a drone and the corresponding ground control station (the flight controller operating by the drone pilot). Second, RF based drone detection must collect features over a wide frequency range to detect a radio communication of UAS. Finally, in a real RF environment, the existence of many other radio signals (e.g. Wi-Fi or Bluetooth) sharing the same frequency band with the UAS, makes RF based detection quite challenging. In (Peacock & Johnstone, 2013), identifying the media access control (MAC) address of a drone is presented as a feasible algorithm. However, this algorithm is only capable of detecting drones with open MAC addresses, because it can be easily spoofed and can provide diverse interpretations. In addition to this, a huge problem can be to create and update a comprehensive dataset containing MAC addresses of all drones, because there is an ever-increasing variety of drones. Some commercial ADRO systems exploit the knowledge of the communication protocols to detect, identify, locate and in some cases hijack (take over) the drone to land it at a predefined location (D-Fend, 2021). An improved solution is the usage of the radio signal's features for drone detection. Based on this, the authors in (Nguyen et al., 2016) proposed a drone detection algorithm based on specific signatures of a drone's body vibration and body shifting that are embedded in the Wi-Fi signal transmitted by a drone. Similarly, RF drone fingerprints (statistical features of a radio signal) with machine learning (ML) algorithms are presented in (Ezuma et al., 2020) for the same objective. However, different techniques like multistage classification, prior RF signal detection, noise removal, or multiresolution analysis were used in this research before ML algorithms to improve detection results. Additionally, drone localization algorithms based on measurements of received signal strength (RSS), time of arrival (TOA), and direction of arrival

(DOA) are applicable with certain restrictions (e.g. multipath and non-line-of-sight propagation). Challenges in RF drone detection (ambient noise or RF background, multipath, etc.) can be an invincible obstacle in some cases causing a large false alarm rate.

### 2.2. Deep learning (DL) algorithms

A respectable ADRO system should have several different types of sensors, i.e. it should be composed of heterogeneous sensor units combined to find application in practice. Such a system, on the other hand, represents a compromise (tradeoff) between well-timed detection, long detection range, high detection probability, and sensor imperfections. It should be noted that the performance of any ADRO system depends on numerous factors: properties of the target (drone dimensions, speed, communication, and navigational system), the surveillance environments (RF traffic density, urban or rural areas, and atmospheric conditions), the hardware parameters (receiver sensitivity, antenna characteristics, OES sensor quality, antenna azimuth, and elevation directivity) and the corresponding algorithms. Using expensive sensors, or combining multiple heterogeneous sensors is not as effective for the detection and identification of drones, as is the usage of a good algorithm. DL algorithms have demonstrated excellent results when applied to different types of problems such as the image object detection and identification in (Krizhevsky et al., 2017; Nair & Hinton, 2009; Pathak et al., 2018), digital signal processing (Peng et al., 2019; Zha et al., 2019; Zhou et al., 2019), radar detection and identification in (Alhadhrami et al., 2019), speech and text recognition in (Karita et al., 2018; Y. Kim, 2014), and in all other areas of everyday life. Furthermore, multimodal DL algorithms presented in (Narkhede et al., 2021; Patel et al., 2015) were presented as novel approaches and implementation for sensor fusion in various applications.

DL algorithms have also found their application in exploiting various data from different sensors to detect and identify drones. Most of these studies include a mandatory step where frequency or time-frequency representation is calculated and saved to an image that is later used as input data for existing DL algorithms already proved in object detection and identification problems. However, there is a small number of related research papers where raw RF data are used as a solution (MathWorks, 2021). Instead of using an image for DNN input data, rudimentary RF signal transformation is performed and the output is then used as a DNN input for RF based DL algorithm.

A comparative analysis of the most recent and prominent studies in the field of detection and identification of drones based on the DL algorithms is shown in Table 1. The analysis was performed on the obtained results as well as the challenges, benefits, and disadvantages of the used algorithms.

It is important to note that the RF detection and identification of the UAS (drones and flight controllers) by using state-of-the-art DL algorithms is the primary objective of all studies that are presented in Table 1. Additionally, the identification of the drone flight modes is examined only in (Al-Emadi & Al-Senaid, 2020; Al-Sa'd et al., 2019) and in this paper. More importantly, all authors used RF signals from 2.4 GHz ISM frequency band for their studies and no one paper presents the 5.8 GHz ISM band research results. Another interesting fact is that only authors in (Abeywickrama et al., 2018; Zhang et al., 2018) investigated scenarios in the outdoor environment. Most of the authors used FFT of raw RF signal (i.e. spectrum matrix) or spectrogram images as DNN input, except in (Zhang et al., 2018). Furthermore, in (Basak et al., 2021), the authors investigated the impact of additive white Gaussian noise (AWGN) and multipath propagation on the DL algorithms accuracy. It is also interesting that in the same work, the authors examined the possibility of detecting multiple drones, but with simulated data. They used previously recorded RF signals (not overlapping in frequency spectrum) from flight controllers, then they artificially summed those signals and created DNN input for multiple drones detection scenarios.

In this paper, the power RF spectrum of the raw radio signal is

**Table 1**

Related works on detection and identification of drones using DL algorithms.

Reference	The proposed algorithm and/or used features	Results [%]	Remarks (challenges, benefits, and disadvantages)
(Al-Sa'd et al., 2019)	<ul style="list-style-type: none"> <li>- Three fully connected Deep Neural Networks (FC-DNN).</li> <li>- DNN input: FFT of raw RF signal (spectrum matrix).</li> </ul>	<ul style="list-style-type: none"> <li>- Detection, type, and flight mode identification</li> <li>- 3 drones with 4 flight modes.</li> <li>- Drone detection accuracy: 99.7%.</li> <li>- Drone type accuracy: 84.5%.</li> <li>- Flight mode accuracy: 46.3%.</li> </ul>	<ul style="list-style-type: none"> <li>- Indoor conditions.</li> <li>- The first study scenario which investigated drone flight mode identification.</li> <li>- Only 2.4 GHz ISM band.</li> <li>- Without noise consideration.</li> </ul>
(Al-Emadi & Al-Senaid, 2020)	<ul style="list-style-type: none"> <li>- Convolutional Neural Network (1-D CNN).</li> <li>- DNN input: FFT of raw RF signal (spectrum matrix).</li> </ul>	<ul style="list-style-type: none"> <li>- Detection, type, and flight mode identification</li> <li>- 3 drones with 4 flight modes.</li> <li>- Drone detection accuracy: 99.8%.</li> <li>- Drone type accuracy: 85.8%.</li> <li>- Flight mode accuracy: 59.2%.</li> </ul>	<ul style="list-style-type: none"> <li>- Indoor conditions.</li> <li>- The dataset from (Al-Sa'd et al., 2019).</li> <li>- The 1-D CNN model outperforms the results from (Al-Sa'd et al., 2019).</li> <li>- Only 2.4 GHz ISM band.</li> <li>- Without noise consideration.</li> </ul>
(Zhang et al., 2018)	<ul style="list-style-type: none"> <li>- Back Propagation Neural Network (BPNN).</li> <li>- DNN input: statistical features (slope, kurtosis, and skewness).</li> </ul>	<ul style="list-style-type: none"> <li>- Drone detection scenario.</li> <li>- N/A drones.</li> <li>- Indoor accuracy: 92.67% within 5 m.</li> <li>- Outdoor accuracy: 82% within 3 km.</li> </ul>	<ul style="list-style-type: none"> <li>- Indoor and outdoor conditions.</li> <li>- The BPNN model outperforms the algorithms based on the statistical features.</li> <li>- Only 2.4 GHz ISM band.</li> <li>- With noise consideration. Empirical mode decomposition (EMD) is used to remove the noise from the RF signal.</li> <li>- Additional consideration: distance from UAS to sensor.</li> </ul>
(Basak et al., 2021)	<ul style="list-style-type: none"> <li>- Deep Residual Neural Network (DRNN).</li> <li>- DNN input: FFT of raw RF signal (spectrum matrix).</li> </ul>	<ul style="list-style-type: none"> <li>- Detection and type identification</li> <li>- 9 drones.</li> <li>- Indoor accuracy: 99.88%.</li> </ul>	<ul style="list-style-type: none"> <li>- Indoor conditions (dataset is recorded in an anechoic chamber).</li> <li>- Multiple drones classification with simulated RF signals (RF signals are artificially added).</li> <li>- Only 2.4 GHz ISM band.</li> <li>- With noise and multipath consideration.</li> <li>- Indoor conditions.</li> </ul>
(Parlin et al., 2020)			

**Table 1 (continued)**

Reference	The proposed algorithm and/or used features	Results [%]	Remarks (challenges, benefits, and disadvantages)
(Abeywickrama et al., 2018)		<ul style="list-style-type: none"> <li>- Convolutional Neural Network (2-D CNN).</li> <li>- DNN input: spectrogram images.</li> </ul>	<ul style="list-style-type: none"> <li>- UAS protocols detection scenario.</li> <li>- 3 UAS protocol types (Taranis, Lightbridge, and Phantom 2).</li> <li>- Indoor accuracy: 97.25%.</li> </ul>
		<ul style="list-style-type: none"> <li>- Sparse denoising autoencoder (SDAE-DNN).</li> <li>- DNN input: the sum of I/Q data from N antennas.</li> </ul>	<ul style="list-style-type: none"> <li>- Direction finding (DF) scenario.</li> <li>- Outdoor accuracy: the worst DF accuracy is 92% for the 180° antenna sector.</li> </ul>

calculated, stored as rows in the matrix (spectrum matrix) which are then used as inputs to the FC-DNN. Experiments were performed in indoor conditions, and DJI's commercial off the shelf (COTS) drones were used. The contribution of this research is in several facts: a new dataset of RF drone signals is made publicly available, multiple drones operating simultaneously were successfully detected, and RF drone signals in 2.4 and 5.8 GHz frequency bands reserved internationally for industrial, scientific, and medical (ISM) purposes were collected and examined.

It is essential to notice that there are currently a small number of publicly available datasets that contain RF drone signals. Because of this, research of various detection and classification algorithms is limited. Also, to the best of our knowledge, no significant open literature research was conducted aiming at the detection of multiple drones using real RF signals (except with radar signals so far). Moreover, the analysis of RF signals from both ISM bands contributed to confirm our preliminary assumptions and comparing the results of detection and identification between different frequency bands.

### 3. Methodology

In this section, the system model is presented. This system model is used to create a new RF drone dataset and to test the detection and identification of single and multiple drones with the proposed DL algorithm.

#### 3.1. System model

For the purposes of this research, the system model used is similar to the model presented in (Al-Sa'd et al., 2019). The similarity is in two main subsystems and corresponding components. These two subsystems are the RF dataset development subsystem and the drone detection and identification subsystem which are shown in Fig. 1.

The main difference from the research explained in (Al-Sa'd et al., 2019) is in the RF dataset development subsystem, because this system model is designated to implement the recordings of new RF drone's data from 2.4 and 5.8 GHz ISM bands. It is important to note that all recordings were performed separately, i.e., first for 2.4 and then for 5.8 GHz ISM band. Besides, the particular and unique scenario (two and three drones operate in the same space and time domain) was recorded in two separate ISM bands. The subsystem for RF drone dataset

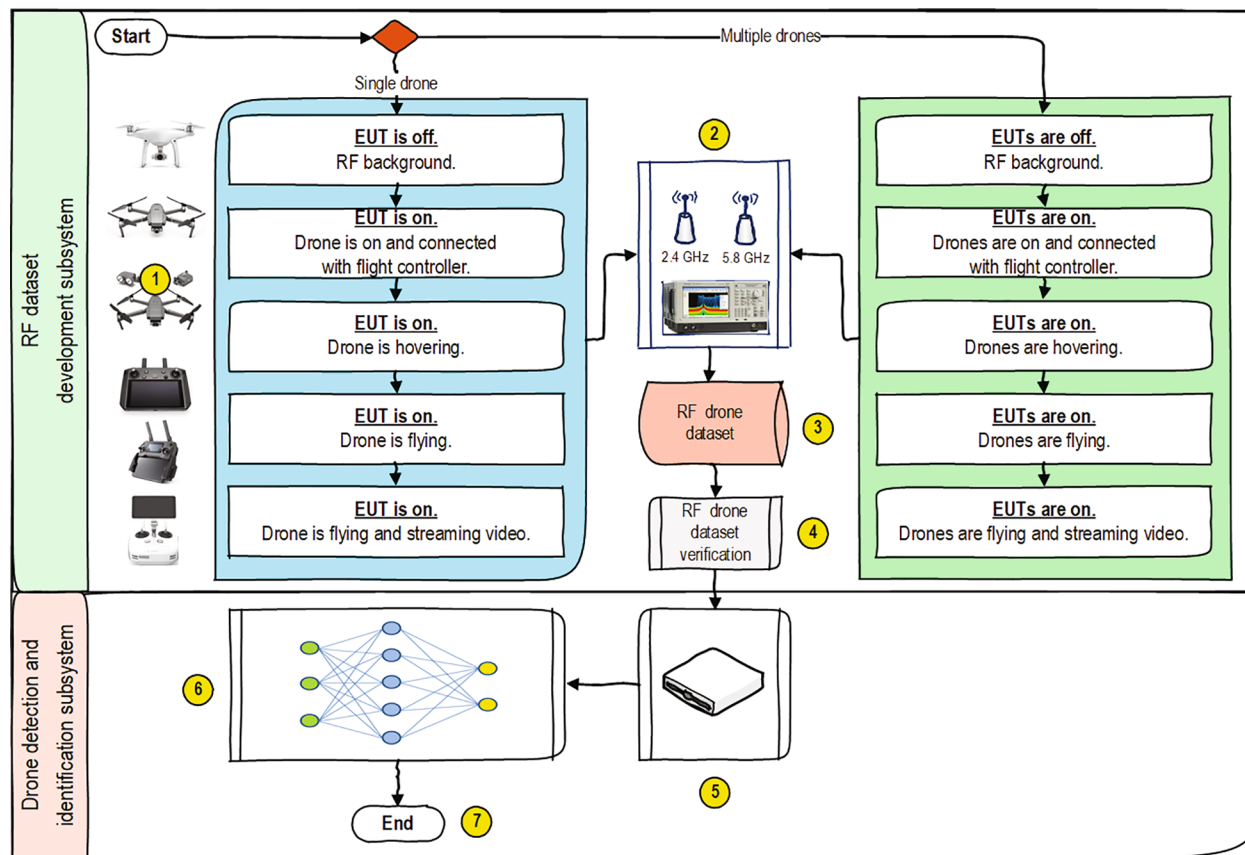


**Fig. 1.** System model: (1) Equipment Under Test (EUT), (2) RF sensor with antennas, (3) RF drone dataset, (4) RF drone dataset verification, (5) RF signal pre-processing and labeling, (6) FC-DNN models, and (7) the system output.

development, which is also described in detail in (Šević et al., 2020), consists of the RF sensor and equipment under test (EUT). For the purpose of the data acquisition and recording, the Tektronix Real-Time

Spectrum Analyzer, two receiving antennas (for two separate ISM bands) with corresponding cables and connectors were used. The Real-Time Spectrum Analyzer instantaneously recorded bandwidth of 110



**Fig. 2.** RF sensor and EUT: a) Tektronix Real-Time Spectrum Analyzer RSA 6120A, b) receiving antennas, c) DJI Phantom IV Pro, d) DJI Mavic 2 Enterprise, and e) DJI Mavic 2 Zoom.

MHz within 2.4 or 5.8 GHz ISM bands and saved records directly in a \*.mat format that is suitable for loading and analyzing in the MatLab application. It is important to notice that the acquisition length of each RF signal was 450 ms and the sampling frequency was 150 MSample/s for instantaneous bandwidth of 110 MHz, which produces a \*.mat file of around 500 MB for every recording in the experiment. Each saved file also contains additional information (metadata) about experiment parameters that can be used after importing into the MatLab application.

### 3.1.1. Equipment under test (EUT)

For the EUT, three different UAS (DJI Phantom IV Pro, DJI Mavic 2 Zoom, and DJI Mavic 2 Enterprise with the corresponding flight controllers) were used (DJI, 2021). Fig. 2 shows Tektronix Real-Time Spectrum Analyzer RSA 6120A with two receiving antennas (for 2.4 and 5.8 GHz ISM bands) and EUT (DJI Phantom IV Pro, DJI Mavic 2 Enterprise, and DJI Mavic 2 Zoom, respectively from left to right).

A drone pilot uses the flight controller to send RF commands to operate the autonomous aircraft by changing flight (operational) modes, altitude (position), and speed. Most drones can operate in 2.4 or 5.8 GHz ISM bands, usually in one or simultaneously in both, when communication is disrupted, automatically or manually adjusted via flight controller.

### 3.2. RF dataset development subsystem

Data acquisition was performed for each drone separately, and each time four distinctive flight (operational) modes were recorded. In order to analyze the whole radio communication traffic, each data acquisition process was organized into five steps:

**EUT is off.** Drone is turned off. RF background (ambient noise) is recorded. For a more genuine approach, random Wi-Fi and Bluetooth radio communications at the beginning were induced.

**EUT is on and performing the connecting procedure with the flight controller.** Drone is turned on by the operator. Drone is connecting to the flight controller. The recording is performed until the drone is connected to the flight controller.

**EUT is hovering.** The operator lifts off the drone and puts it in a state of hovering (the drone is flying without altering altitude and position, i.e., the operator is not giving any commands). The recording is performed while the drone is hovering (maintaining height and position) without any operator commands.

**EUT is flying.** The operator issues some basic commands while the drone is moving left, right, down, and up. The recording is performed while the drone is flying (the drone is changing the altitude and position all the time) following the commands from the operator.

**EUT is flying and recording a video.** The operator enables a video recording on the drone and issues some basic commands while the drone is moving left, right, down, and up. The recording is performed while the drone is flying and the video is being transmitted and recorded to the flight controller.

This step-by-step procedure was done for all drones and constitute one experiment. Firstly, three experiments were executed, one with each drone, one with two drones, and one with three drones, with 25 recordings in total (15 recordings for the first experiment, 5 recordings for the second, and 5 recordings for the third experiments) in 2.4 GHz ISM band. Then, the whole procedure was repeated for 5.8 GHz ISM band, with another 25 recordings (or 50 recordings in total). Again, it is important to point out that each experiment was conducted in laboratory (indoor) conditions where the RF background recording was firstly executed.

The final stage of the RF dataset development subsystem was to perform time-frequency analysis (TFA) in the MatLab application over-collected raw RF drone signals to verify the RF drone dataset (see Fig. 1). MatLab embedded spectrogram function based on Short-Time Fourier Transform (STFT) was used as one of TFA's basic tools before the drone detection and identification subsystem was engaged. The primary

objective of the verification stage of the RF drone dataset was to check out if it is possible to visually differentiate types of drones and types of flight modes in the calculated spectrograms. The secondary objective was to determine the elementary physical characteristics of the RF drone signals such as signal type (fixed frequency signal, frequency hopping signal, signal with direct sequence or burst), total channel number, channel central frequency, channel bandwidth, total channels (occupied bandwidth), channel raster (frequency distance between channels), hop duration and dwell time for each drone's recording (see [supplementary material](#)). As a result, all three types of drones and their operational modes were successfully differentiated. These results were not used as an input for FC-DNN models, but just for checking out the consistency of the RF drone dataset.

Examples of spectrograms calculated from the recorded RF activities in 2.4 GHz ISM band are shown in the following figures. In the beginning, as an illustration, Fig. 3 provides a detailed explanation of all the components on the spectrogram of the RF drone signal, to better understand the basic method of the drone operation.

Two distinguished components can be seen in Fig. 3: the uplink for command-and-control signals and the downlink for the video signal. The uplink for command-and-control signals is marked with black circles, while the downlink for the video signal is marked with a blue rectangle. It is unambiguous that the downlink is a fixed frequency emission (the central frequency does not change during the operation) and the uplink is a frequency hopping emission (the central frequency changes according to a predefined rule during the operation). All spectrograms of all drones that were part of the experiments are shown in the [supplementary material](#).

Further, Fig. 4 shows the spectrograms of one drone with four distinctive flight modes, Fig. 5 illustrates spectrograms of a single mode of operation for different drones, and finally, Fig. 6 presents snapshots of the situation when multiple drones (two and three) operate simultaneously.

Moreover, several additional facts were established which can be of interest in further studies: all three drones operate in a designated frequency range which is defined by DJI, all three drones use the spread spectrum (SS) technique based on frequency hopping (FH) for communication between drone and flight controller, and the drone's FH emission is very simple and comparable to sweep signals. Also, it is interesting to note that DJI Phantom IV Pro has the same principle of FH emission in all operational (flight) modes (see [supplementary material](#)).

### 3.3. Drone detection and identification subsystem

The second part of the system model – the drone's detection and identification subsystem, remained similar as in (Al-Sa'd et al., 2019) and the three FC-DNN models were used to verify the consistency of the new RF drone dataset (on the subject of drone detection, drone identification, and drone type and flight mode identification). The additional, fourth FC-DNN model for multiple drones detection is the crucial difference introduced in this paper. Also, there were made slight changes in the data labeling procedure to validate the possibility to detect situations when two or three drones operate concurrently.

#### 3.3.1. Signal preprocessing

The custom-made MatLab functions were used to perform signal preprocessing and labeling steps, required for necessary data preparation. Such data were intended to be used as an input to FC-DNN models. In order to preprocess and prepare raw data obtained from the first part of the system model, signal segmentation and simple calculation of the power RF spectrum were performed for each segment of signals in both ISM bands. The signal segmentation was performed by dividing the whole acquired RF signal into snapshots of data consist of 100.000 samples. This process was performed to speed up signal preprocessing and to perform data augmentation because each segment of each RF signal was used as an FC-DNN input. It is important to emphasize that

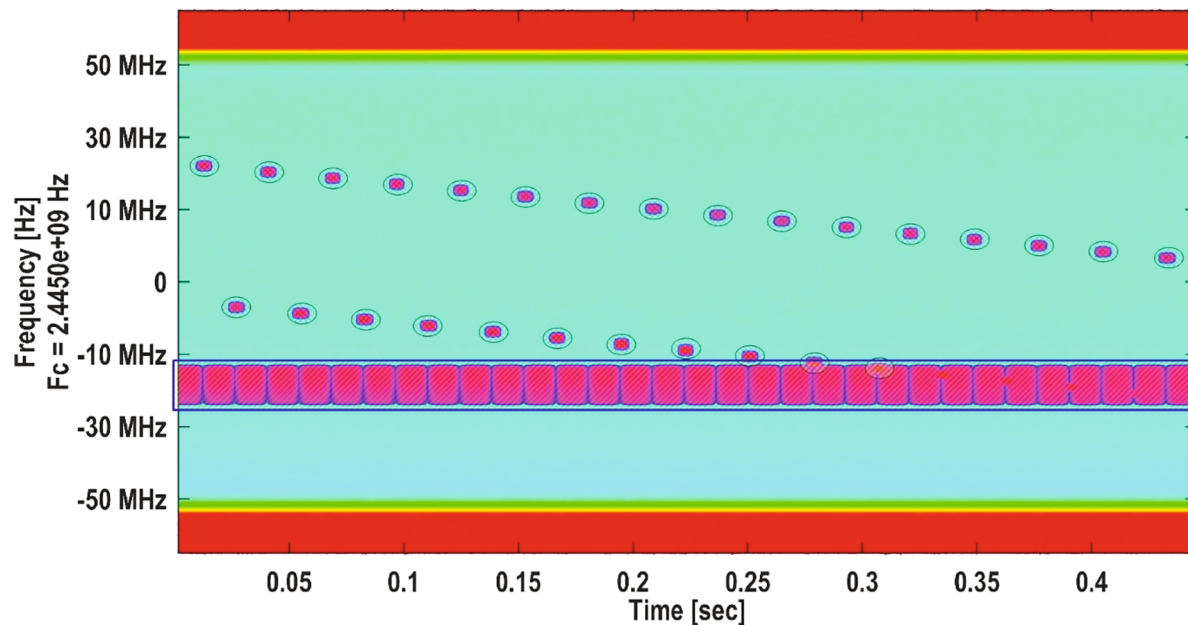


Fig. 3. Characteristic elements on the spectrogram of the RF drone signal.

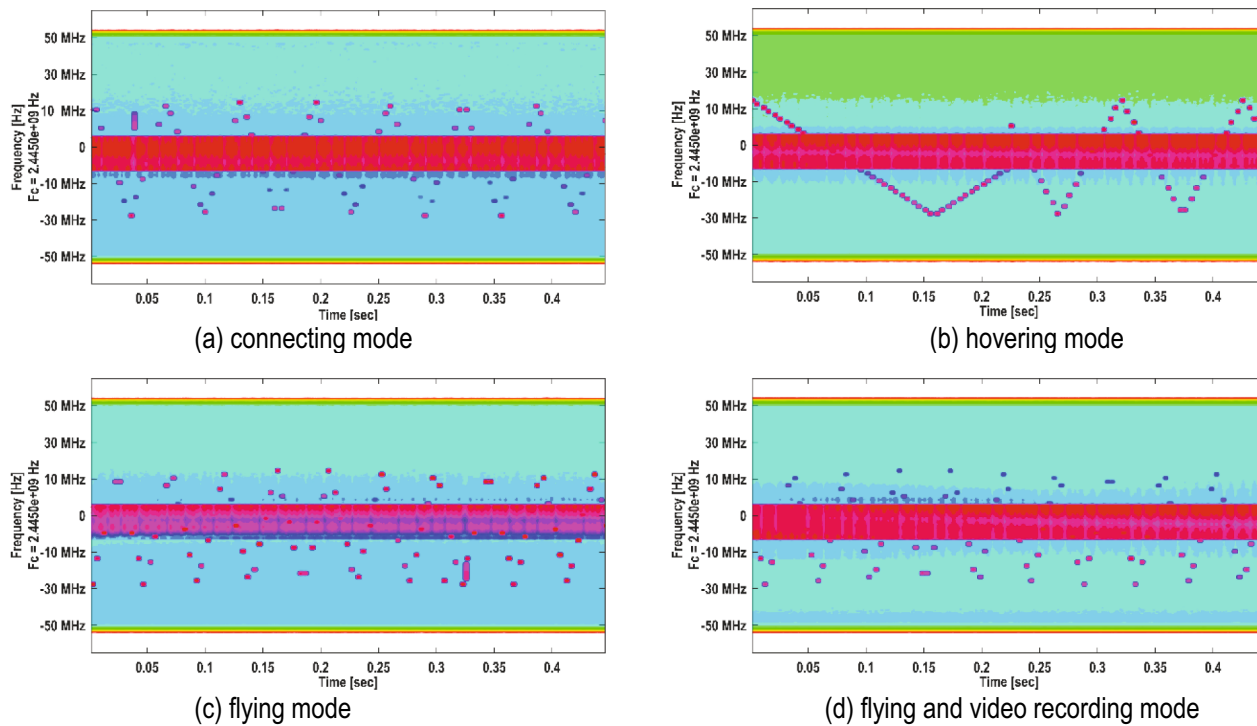


Fig. 4. RF spectrograms of DJI Mavic 2 Enterprise in 2.4 GHz ISM band.

simple signal segmentation without overlapping windows and without discarding noisy segments (segments without useful signal) was used in this research. Moreover, data augmentation and accuracy of the FC-DNN model can be improved by using an overlapping window for signal segmentation, as well as with discarding segments where there is only noise (e.g. between two hops). For power RF spectrum calculation, a modified built-in MatLab function (pspectrum) was used with 2048 frequency bins without the DC component of the RF signal (zero mean option). This function finds a compromise between the spectral resolution achievable with the entire length of the signal and the performance

limitations that result from computing large FFT (MathWorks, 2021).

Additionally, data scaling of FC-DNN inputs as a recommended preprocessing step was performed by using the normalization technique (to rescale input variables before training a neural network model in the range of zero to one).

Subsequently, data aggregation (preprocessed and labeled RF signals from all experiments) was performed and the results are stored in four matrices (two matrices for 2.4 GHz and two for 5.8 GHz ISM bands representing the power RF spectrum). FC-DNN's input data specification is presented in detail in Table 2.

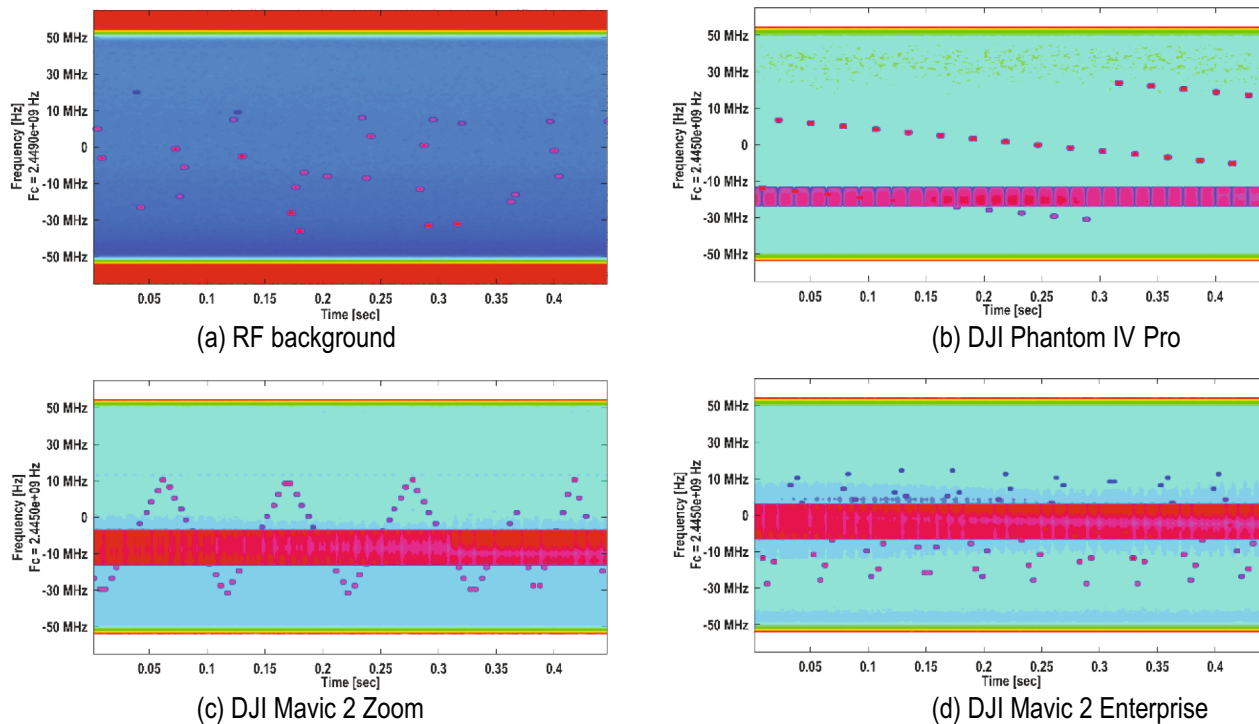


**Fig. 5.** RF spectrograms for RF background and flying and video recording mode of different drones in 2.4 GHz ISM band.

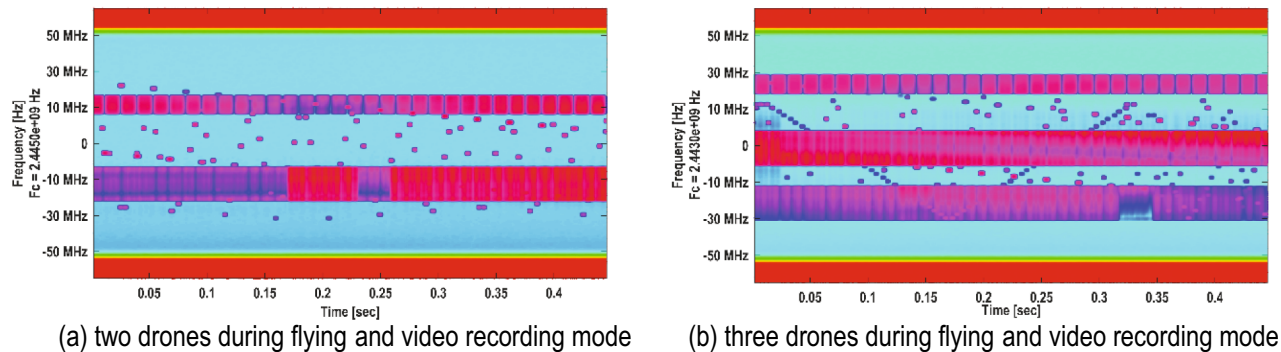


**Fig. 6.** RF spectrograms when multiple drones (two and three) operate simultaneously in 2.4 GHz ISM band.

**Table 2**  
FC-DNN's input data specifications.

		Experiment No.1 (single drone)	Experiment No.2 (two drones)	Experiment No.3 (three drones)
RF signal	Segments No.	670 segments	670 segments [2048 × 670]	670 segments [2048 × 670]
	Resulting matrix	[2048 × 670]		
2.4 GHz ISM band	Signals No.	15 signals	5 signals	5 signals
	Segments No.	15 × 670 segments		
2.4 GHz input data	Resulting matrix	[2048 × 10,050]	5 × 670 segments [2048 × 3350]	5 × 670 segments [2048 × 3350]
	Concatenated matrix (FC-DNN input)	2.4 GHz input matrix FC-DNN No. 1, 2, 3 [2048 × 10,050]		
5.8 GHz ISM band	Signals No.	15 signals	2.4 GHz input matrix FC-DNN No. 4 [2048 × 16750] (also consist data from the first experiment)	5 signals
	Segments No.	15 × 670 segments		
	Resulting matrix	[2048 × 10,050]		
5.8 GHz input data	Concatenated matrix (FC-DNN input)	5.8 GHz input matrix FC-DNN No. 1, 2, 3 [2048 × 10,050]	5.8 GHz input matrix FC-DNN No. 4 [2048 × 16750] (also consist data from the first experiment)	5 signals

It must be mentioned that each concatenated matrix from the first experiment was used as an input in the first three DNN models for solving detection and identification problems. Additionally, all concatenated matrices from all the experiments were used as an input in the fourth FC-DNN model for solving the multiple drones detection problem.

### 3.3.2. Data labeling

Labeling for all FC-DNN models was performed by adding rows at the end of the corresponding aggregated matrices. For detection and identification purposes, rows that were added to the concatenated matrices from the first experiment are as follows: the first row is consisted of labels for detection of drones, the second row is consisted of labels for drone's type identification, and the third row is consisted of labels for drone's flight mode identification. For the detection of multiple drones, the same labeling principle was used, but one more row of labels was added. It should be perceived that labels in each row determine whether the signal's segment (matrix column) represents the RF background, the presence of a drone, or another specific situation (the type of drone, flight mode of drone, or presence of multiple drones).

To prepare FC-DNN input data and to create a new RF drone dataset, a Binary Unique Identifier (BUI) proposed in (Al-Sa'd et al., 2019) was used for data notation. The good practice was followed and the new RF drone dataset was created using suggested parameters such as the number of experiments (E), the total number of drones (D), and the total number of flight modes, including RF background (F). Finally, a new dataset was completed by using E = 3, D = 3 and F = 5. Details of this RF drone dataset showing the number of segments for each class relative to the used FC-DNN models are presented in Table 3.

Based on the presented specification of the RF drone dataset, data labeling was performed for detection and identification purposes for different FC-DNN:

**Drone detection.** The first FC-DNN model uses a data label for the presence of drone detection. This label represents the drone absence class with "1" and presence with "2". All recorded data from the first experiment were used.

**Drone type identification.** The second FC-DNN model uses a data label for drone type identification. This label contains four different designations: "1" – RF background, "2" – DJI Phantom IV Pro, "3" – DJI Mavic 2 Zoom, and "4" – DJI Mavic 2 Enterprise. Like in the previous case, all recorded data from the first experiment were used.

**Drone type and flight (operational) mode identification.** The third FC-DNN model uses a data label for drone type identification. This label contains thirteen different designations: "1" – RF background, "2" – DJI Phantom IV Pro connected, "3" – DJI Phantom IV Pro hovering, "4" – DJI Phantom IV Pro flying, "5" – DJI Phantom IV Pro flying and recording video, "6" – DJI Mavic 2 Zoom connected, "7" – DJI Mavic 2 Zoom hovering, "8" – DJI Mavic 2 Zoom flying, "9" – DJI Mavic 2 Zoom flying and recording video, "10" – DJI Mavic 2 Enterprise connected, "11" – DJI Mavic 2 Enterprise hovering, "12" – DJI Mavic 2 Enterprise flying, and "13" – DJI Mavic 2 Enterprise flying and recording video. For drone type and flight mode identification purposes, recorded data from the first experiment were used.

**Drone number detection.** The fourth FC-DNN model uses a data label for the number of drone detection. This label contains four different descriptions: "1" – RF background, "2" – one active drone, "3" – two active drones, and "4" – three active drones. Recorded data from all experiments were used.

### 3.3.3. FC-DNN model

After the signal preprocessing and data labeling, the detection and identification of the drones were performed. The supervised DL algorithm was engaged with four FC-DNN models where each one is consisted of an input layer, hidden layers, and an output layer. The fundamental building block of each FC-DNN (i.e. feedforward neural networks) is the fully-connected neuron, which can be defined by the formula (Winovich, 2021):

**Table 3**  
Specification of RF drone dataset for one ISM band.

FC-DNN model No.	Class name	Class label	Signal No.	Segments No. (100000 samples)	Ratio [%]
1	No drone (RF background)	"1"	3	2010	20.00
2	Drone	"2"	12	8040	80.00
	No drone (RF background)	"1"	3	2010	20.00
	DJI Phantom IV Pro	"2"	4	2680	26.67
	DJI Mavic 2 Zoom	"3"	4	2680	26.67
	DJI Mavic 2 Enterprise	"4"	4	2680	26.67
3	No drone (RF background)	"1"	3	2010	20.00
	DJI Phantom IV Pro flight mode 1	"2"	1	670	6.67
	Flight mode 2	"3"	1	670	6.67
	Flight mode 3	"4"	1	670	6.67
	Flight mode 4	"5"	1	670	6.67
	DJI Mavic 2 Zoom flight mode 1	"6"	1	670	6.67
	Flight mode 2	"7"	1	670	6.67
	Flight mode 3	"8"	1	670	6.67
	Flight mode 4	"9"	1	670	6.67
	DJI Mavic 2 Enterprise flight mode 1	"10"	1	670	6.67
	Flight mode 2	"11"	1	670	6.67
	Flight mode 3	"12"	1	670	6.67
	Flight mode 4	"13"	1	670	6.67
4	No drone (RF background)	"1"	5	3350	20.00
	One drone	"2"	12	8040	48.00
	Two drones	"3"	4	2680	16.00
	Three drones	"4"	4	2680	16.00

$$y = f \left( \sum_j \omega_j x_j + b \right) \quad (1)$$

where  $x_j$  is input to the neuron,  $\omega_j$  are weights,  $b$  is bias,  $j$  is input size,  $f$  is activation function, and  $y$  is output. Combining multiple neurons, it is possible to create a simple fully-connected neural network that is consisted of input, one intermediate (so-called hidden), and output layers. The result of hidden layer values is given by:

$$y_i = f \left( \sum_j \omega_{i,j} x_j + b_i \right) \quad (2)$$

where  $j$  is the size of the input layer and  $i$  is the size of the hidden layer.

The final output from this shallow fully-connected neural network,  $z$  is the sum of all results obtained from the hidden layer, thus it is presented as:

$$z = f \left( \sum_l \omega_l^{(z)} y_l + b^{(z)} \right) \quad (3)$$

where  $l$  is the number of hidden layers and  $b^{(z)}$  refers to weights and biases values from the corresponding layer. Using matrix notation these equations can be expressed more concisely. For example, underlying mathematical relations for FC-DNN with two hidden layers are shown with the following equations:

$$\mathbf{y}^{(1)} = f(\mathbf{W}^{(1)} \mathbf{x} + \mathbf{b}^{(1)}) \quad (4)$$

$$\mathbf{y}^{(2)} = f(\mathbf{W}^{(2)} \mathbf{y}^{(1)} + \mathbf{b}^{(2)}) \quad (5)$$

$$z = f(\mathbf{W}^{(z)} \mathbf{y}^{(2)} + \mathbf{b}^{(z)}) \quad (6)$$

Equations (4), (5), and (6) denote the results obtained from the first, the second, and the output layer, respectively.

Accordingly, the proposed FC-DNN models can be described with the following input-output relations (Al-Sa'd et al., 2019):

$$\mathbf{z}_i^{(l)} = f^{(l)}(\mathbf{W}^{(l)} \mathbf{z}_i^{(l-1)} + \mathbf{b}^{(l)}) \quad (7)$$

where  $i$  is the number of input RF segment;  $\mathbf{z}_i^{(0)} = \mathbf{y}_i$  is the power spectrum of  $i$ -th input RF segment;  $\mathbf{z}_i^{(l-1)}$  is the output of the layer  $l-1$  and the input to the layer  $l$ ;  $\mathbf{z}_i^{(l)}$  is the output of the layer  $l$  and the input to the layer  $l+1$ ;  $\mathbf{z}_i^{(L)} = \mathbf{c}_i$  is the classification vector for  $i$ -th input RF segment;  $\mathbf{b}^{(l)} = [b_1^{(l)}, b_2^{(l)}, \dots, b_{H^{(l)}}^{(l)}]^T$  is the bias vector of layer  $l$ ;  $f^{(l)}$  is the activation function of layer  $l$  ( $l = 1, 2, \dots, L$  and  $L-1$  is the total number of hidden layers). Also, the weight matrix of layer  $l$  is designated as  $\mathbf{W}^{(l)}$ :

$$\mathbf{W}^{(l)} = \begin{bmatrix} w_{11}^{(l)} & \cdots & w_{1H^{(l-1)}}^{(l)} \\ \vdots & \ddots & \vdots \\ w_{H^{(l)}1}^{(l)} & \cdots & w_{H^{(l)}H^{(l-1)}}^{(l)} \end{bmatrix} \quad (8)$$

where  $w_{ij}^{(l)}$  is the weight between the  $i$ <sup>th</sup> neuron of layer  $k$  and  $j$ <sup>th</sup> neuron of layer  $l-1$ ;  $H^{(l)}$  is the total number of neurons in layer  $l$ ;  $H^{(0)} = M = 2048$ ; and  $H^{(L)} = C$  is the number of classes in the classification vector  $\mathbf{c}_i$ .

It is important to notice that each FC-DNN model in the proposed algorithm has similar core architecture. Each FC-DNN model consists of an input layer, hidden layers, and an output layer. Hidden layers can be grouped in three separate sets, where each one consists of two fully-connected (dense) layers with the rectified linear unit (ReLU) and the sigmoid activation function. Moreover, it is significant to emphasize that fully-connected layers in the first, the second, and the third set of hidden

layers are consist of 256, 128, and 64 neurons, respectively. Comparing to the original FC-DNN model introduced in (Al-Sa'd et al., 2019), which had only three fully-connected hidden layers with ReLU activation function, this is an enhancement. This can be elicited by Fig. 7 that shows an example of the fourth FC-DNN model used for multiple drones detection.

The input layer of the fourth FC-DNN model is the size of the power RF spectrum calculated with 2048 frequency bins. Next, hidden layers organized in three sets of hidden layers are engaged. Although unusual, a combination of two activation functions was used for each set of hidden layers in the FC-DNN model. The sigmoid function is affected by saturation issues which are explained in (Manessi & Rozza, 2018), so the ReLU function is engaged to overcome such weakness and improve the accuracy results of FC-DNN. Finally, the output layer of the fourth FC-DNN is the fully-connected output layer of four neurons with the Soft-Max activation function. For training and validation process following FC-DNN parameters during experiments were used: stochastic gradient descent (SGD) optimization algorithm with backpropagation for the error minimization that uses a training dataset to update a model, Adam optimizer (Zhong et al., 2020) for the classification mean square error minimization, stratified K-fold cross-validation ( $K = 10$ ) for the bias minimization (to overcome the difference between classes); hyperparameter of SGD that controls the number of training samples (batch size = 20), and hyperparameter of SGD that controls the number of complete passes through the training dataset (total number of epochs = 100).

### 3.4. Implementation

For implementation purposes, the proposed FC-DNN models with Python Anaconda version 1.9.2 with Tensorflow 2.1.0 (including Keras 2.3.0) framework and GPU environment setup were used. The host machine for this purpose was Intel(R) Core (TM) i5-9400F CPU @ 2.90 GHz, 32 GB RAM with two GPUs GeForce RTX 2060 6 GB GDDR6 (CUDA toolkit version 10.1. and cuDNN version 7.6). Existing FC-DNNs were modified according to the specification of the RF drone dataset and created four FC-DNNs using Keras to perform the following tasks: to detect the presence of a drone, to detect the presence of a drone and identify its type, to detect the presence of a drone, identify its type, and

**Table 4**  
Average elapsed time for necessary calculations.

Preprocessing stage	FC-DNN No. 1	FC-DNN No. 2	FC-DNN No. 3	FC-DNN No. 4
Average elapsed time [sec]	0.254251	0.052186	0.057668	0.052373

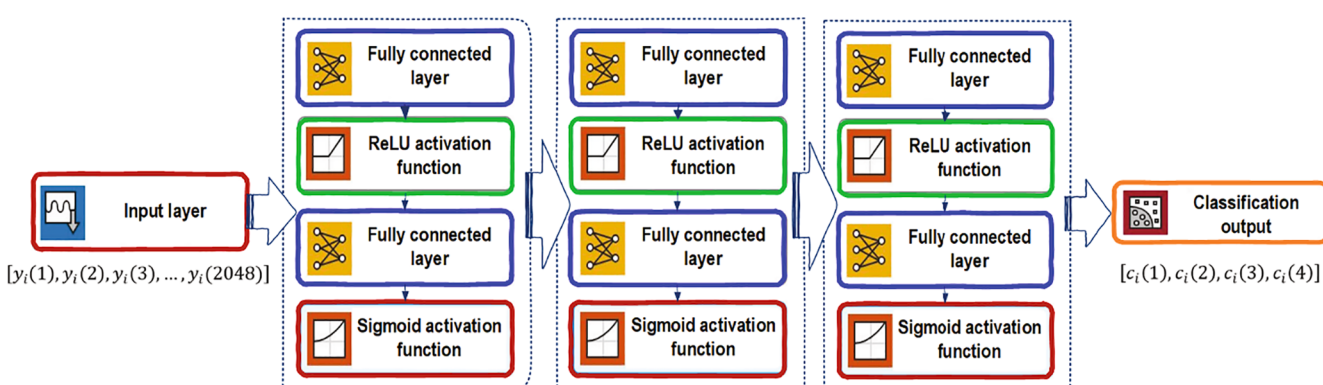


**Fig. 7.** The fourth FC-DNN structure and settings.

determine its flight mode, and lastly, to detect the presence of a drone and identify the number of drones. Also, real-time testing was performed with the proposed algorithm. The average computing time of the proposed system workflow was measured for each FC-DNN model and presented in Table 4.

It should be noted that the average time required to execute the proposed algorithm on the host machine was obtained through a simulation with 100 segments from three different newly captured RF signals. The obtained times for the classification purposes are similar for all FC-DNN models, but the time necessary for the preprocessing stage is almost 5 times bigger. The results from Table 4 show that it is possible to detect/identify the drone from the received RF signal within only 0.31 s (sum of the first and one of the rest columns). It should be emphasized that this is a respectable outcome even though the preprocessing stage was not implemented on the GPU platform, rather only trained FC-DNN models. Based on all the above, a workflow graphic representation of the proposed algorithm is given in Fig. 8.

Workflow graphic representation represents a detailed description of the drone detection and identification subsystem consisted of FC-DNN data preparation, training, and real-time classification on a pre-trained model. FC-DNN data preparation is the first phase of the workflow of the proposed algorithm and can be defined as the following step-by-step procedure: loading data from the RF drone dataset, signal segmentation, spectrum calculation, aggregation of data, and data labeling. Labeled data are afterward handled by FC-DNN models for the training process and the trained models are finally obtained and saved for the real-time simulation of drone detection and identification. It should be noted that four separate FC-DNN models were intentionally used for training and testing phases. The main reason for such odd implementation is to satisfy the demand of the ADRO system's tactical demands. The request was to develop independent classifiers for single and multiple drones detection and identification. Because of that, the introduced problem

was divided into several smaller ones (detection, type identification, flight mode identification, and drone number detection), which were solved using four separate FC-DNN models.

#### 4. Results and discussions

The main goal of this research was to create a new RF drone dataset and to analyze the application possibilities of the RF based DL algorithms in drone detection and identification. In addition, the results of the multiple drones detection and identification system are presented and discussed.

Performance assessment of the RF based ADRO system is represented with accuracy, precision, recall, error, false discovery rate (FDR), false-negative rate (FNR), and F1 scores via appropriate confusion matrices (Al-Sa'd et al., 2019). To better understand the performance of FC-DNN models in such a way, an example of a confusion matrix for two classes with an explanation of corresponding rows, columns, and cells is presented in Fig. 9.

Next, in Figs. 10 and 11, the overall results of the performance assessment of the RF based drone's detection and identification system for both ISM bands are presented. This is convenient because it is easy to compare the results of detection and identification of drones in 2.4 or 5.8 GHz ISM bands. Also, TensorFlow tracking and visualizing metrics such as loss and accuracy during the training process were presented in the form of graphs (see the supplementary material).

First of all, Fig. 10 (a) and (b) shows the classification performance of the first FC-DNN model which detects the presence of a drone in 2.4 and 5.8 GHz ISM bands, respectively. The results present an average accuracy of 98.6% and an average F1 score of 97.8% for 2.4 GHz ISM band, and an average accuracy of 99.8% and an average F1 score of 99.6% for 5.8 GHz ISM band. The absolute error of the average accuracy between the ISM bands for the first DNN model is 1.2%.

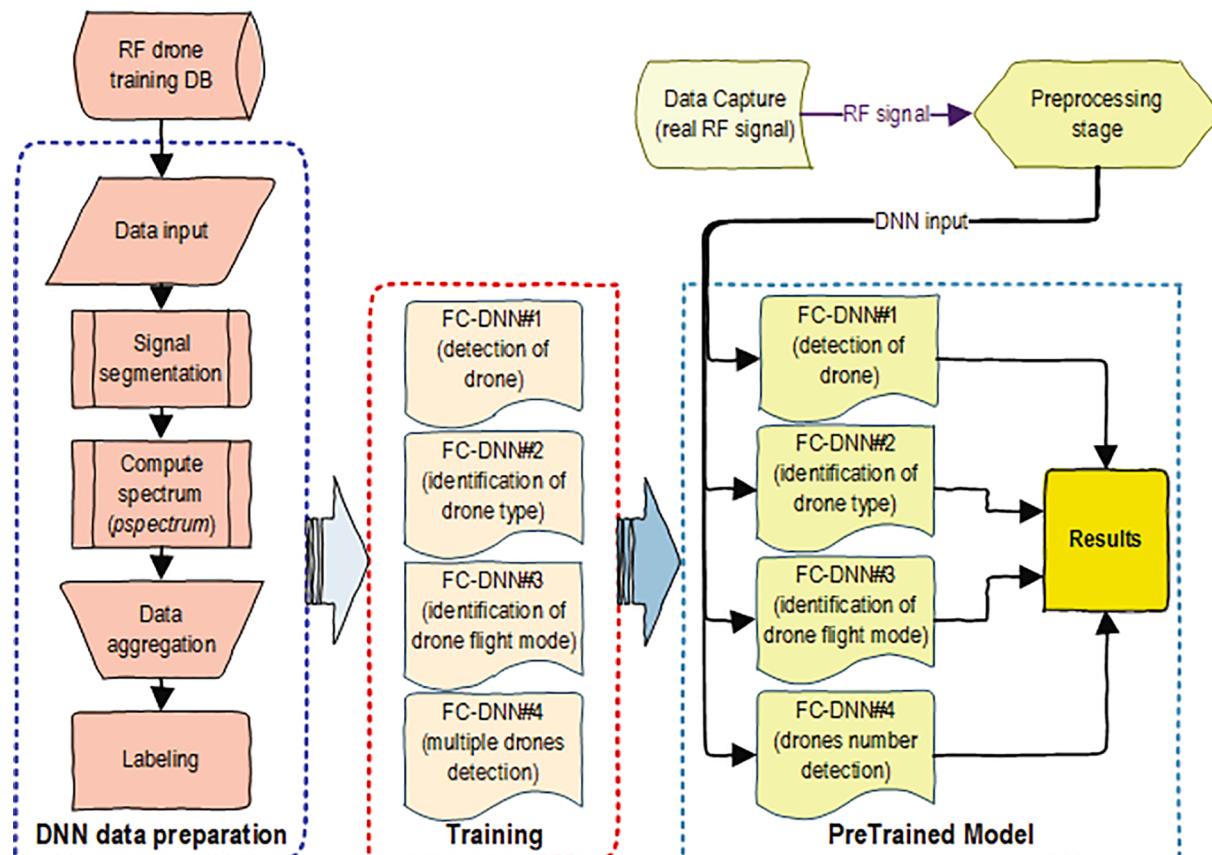


Fig. 8. Flow chart of the proposed algorithm.

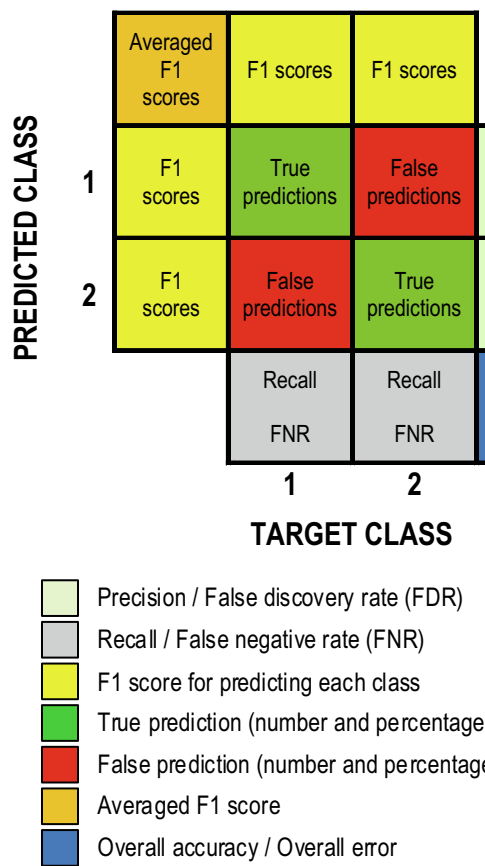


Fig. 9. Resultant rows, columns, and cells for confusion matrix with an explanation.

Secondly, Fig. 10 (c) and (d) illustrate the classification performance of the second FC-DNN model which detects the presence of a drone and identifies its type in 2.4 and 5.8 GHz ISM bands, respectively. The results present an average accuracy of 96.1% and an average F1 score of 96.0% for 2.4 GHz ISM band, and an average accuracy of 95.7% and an average F1 score of 95.8% for 5.8 GHz ISM band. The absolute error of the average accuracy between the ISM bands for the second FC-DNN model is 0.4%.

Thirdly, Fig. 11 illustrates the classification performance of the third FC-DNN model which detects the drone type and determines its flight (operational) mode in 2.4 and 5.8 GHz ISM bands, respectively. The results demonstrate an average accuracy of 85.9% and an average F1 score of 84.2% for 2.4 GHz ISM band, and an average accuracy of 86.9% and an average F1 score of 85.3% for 5.8 GHz ISM band. The absolute error of the average accuracy between the ISM bands for the third FC-DNN model is 1.0%.

Finally, Fig. 12 illustrates the classification performance of the fourth FC-DNN model, which was used for the detection of the drone's presence and the number of detected drones in 2.4 and 5.8 GHz ISM bands, respectively.

The results in Fig. 12 demonstrate an average accuracy of 96.2% and an average F1 score of 96.4% for 2.4 GHz ISM band, and an average accuracy of 97.3% and an average F1 score of 96.8% for 5.8 GHz ISM band. The absolute error of the average accuracy between the ISM bands for the fourth FC-DNN model is 1.1%.

The performance of all FC-DNN models is stable for both ISM bands, as the maximal absolute error for average accuracy is 1.2% for assessment of the RF based drone's detection problem. Notwithstanding, a simple evaluation of the obtained results still leads to the fact that the average accuracy is marginally better for the 5.8 GHz ISM band.

It should be emphasized that to the best of our knowledge this is the

first paper that has presented and explained detection and identification in both ISM bands. More importantly, a new FC-DNN model was constructed, and thereafter its performance was tested with this new RF drone dataset. The created system model is showing respectable results in multiple drones detection, which is also unique research especially in the RF domain.

Moreover, we have compared the proposed algorithm with CNN and Long Short-Term Memory (LSTM) deep learning algorithms. Correspondingly, the DL algorithms from the literature were engaged with our RF drone dataset with the same objective. Outcomes from this comparative analysis are presented in Table 5.

First of all, three representatives from CNN algorithms (AlexNet, ResNet-18, and SqueezeNet) were engaged and showed promising outcomes but still below obtained results with the proposed algorithm. These representatives provide better results for multiple drones number detection for 2.4 GHz ISM band (for example, AlexNet achieved 1.2% better results than the proposed approach). Also, these representatives provide better results for flight mode identification in 2.4 GHz ISM band (for example ResNet-18 achieved 4.8% better results). Nevertheless, the proposed approach succeeded to accomplish better in all other scenarios in both ISM bands. The proposed algorithm has stable detection and identification results in both ISM bands, in contrast to these three representatives where the results in the 5.8 GHz band are significantly worse than the results in the 2.4 GHz band.

Second, the LSTM algorithm was engaged with the same objective, but it achieved worse results than the proposed algorithm in all scenarios in both ISM bands. Notwithstanding, LSTM can be a supportive algorithm because it uses the same data (spectrum matrix) input as the proposed algorithm.

Third, two DL algorithms from the literature were used for comparison using our RF drone dataset, and one of them is proposed for detection purposes only (Parlin et al., 2020). The proposed algorithm outperformed both DL algorithms from the literature.

Finally, two ML algorithms from the literature are also engaged to compare the proposed DL algorithm's effectiveness over some conventional methods. The features extraction procedure used for this purpose is based on (Ezuma et al., 2020) and executed within our dataset. After the feature extraction, 15 statistical descriptors were obtained and used as input for the k-nearest neighbor (kNN) and the Support Vector Machine (SVM) ML algorithms. The best result was achieved with the kNN algorithm (the number of neighbors is 20, the distance metric is Chebyshev, and the distance weight is squared inverse). Nevertheless, this result is still worse than the proposed FC-DNN models.

It is important to emphasize that conditions of experiments should be taken into consideration during the comparison of the results from Table 5. To the best of our knowledge, there are no researchers that exploit CNN (AlexNet, ResNet-18, and SqueezeNet) or LSTM algorithms for the RF detection of drones, so the corresponding fields in Table 5 are empty. Additionally, some authors did not consider all of the presented problems from this paper, but only drone detection or identification. Of particular note are excellent results for the identification of drone controllers obtained via ML algorithms and presented in (Ezuma et al., 2020). However, these results were obtained after a Markov model-based naïve Bayes decision mechanism (for RF signals detection), which was followed by the kNN algorithm (only for drone controllers identification). It is worth mentioning that the proposed algorithm achieved slightly worse accuracy but without multistage classification, prior RF signal detection, noise removal, or multiresolution analysis.

In general, based on the obtained results, the following conclusions can be pointed out:

The average accuracy of the RF background detection persists at a high rate for all FC-DNNs in both ISM bands. This can be explained by the fact that all experiments were conducted in indoor conditions. Moreover, the accuracy of the drone detection would be reduced by performing all experiments in outdoor conditions, because the signal-to-noise ratio (SNR) would be lower and the impact of interference greater.

		Predicted Class		Target Class	
		1	2	1	2
		1	2	1	2
Predicted Class	1	97.8% 2.2%	96.6% 3.4%	99.1% 0.9%	
	2	96.6% 3.4%	2010 20.0%	143 1.4%	93.4% 6.6%
Target Class	1	99.1% 0.9%	0 0.0%	7897 78.6%	100% 0.0%
	2	100% 0.0%	98.2% 1.8%	98.6% 1.4%	

(a) drone detection with 2 classes in 2.4 GHz

		Predicted Class		Target Class	
		1	2	1	2
		1	2	1	2
Predicted Class	1	99.6% 0.4%	99.4% 0.6%	99.8% 0.2%	
	2	99.4% 0.6%	2010 20.0%	25 0.2%	98.8% 1.2%
Target Class	1	99.8% 0.2%	0 0.0%	8015 79.8%	100% 0.0%
	2	100% 0.0%	99.7% 0.3%	99.8% 0.2%	

(b) drone detection with 2 classes in 5.8 GHz

		Predicted Class					
		1	2	3	4	1	2
		1	2	3	4	1	2
Predicted Class	1	96.0% 4.0%	93.3% 6.7%	96.5% 3.5%	97.1% 2.9%	97.0% 3.0%	
	2	93.3% 6.7%	2008 20.0%	146 1.5%	54 0.5%	88 0.9%	87.5% 12.5%
Target Class	1	96.5% 3.5%	0 0.0%	2521 25.1%	22 0.2%	2 0.0%	99.1% 0.9%
	2	97.1% 2.9%	0 0.0%	11 0.1%	2571 25.6%	34 0.3%	98.3% 1.7%
Predicted Class	3	97.0% 3.0%	2	2	33 0.3%	2556 25.4%	98.6% 1.4%
	4	99.9% 0.1%	94.1% 5.9%	95.9% 4.1%	95.4% 4.6%	96.1% 3.9%	

(c) drone type identification with 4 classes in 2.4 GHz

		Predicted Class					
		1	2	3	4	1	2
		1	2	3	4	1	2
Predicted Class	1	95.8% 4.2%	97.1% 2.9%	95.8% 4.2%	93.7% 6.3%	96.6% 3.4%	
	2	97.1% 2.9%	1932 19.2%	0 0.0%	28 0.3%	7 0.1%	98.2% 1.8%
Target Class	1	95.8% 4.2%	0 0.0%	2578 25.7%	72 0.7%	52 0.5%	95.4% 4.6%
	2	93.7% 6.3%	65 0.6%	89 0.9%	2573 25.6%	86 0.9%	91.5% 8.5%
Predicted Class	3	96.6% 3.4%	13 0.1%	13 0.1%	7 0.1%	2535 25.2%	98.7% 1.3%
	4	96.1% 3.9%	96.2% 3.8%	96.0% 4.0%	94.6% 5.4%	95.7% 4.3%	

(d) drone type identification with 4 classes in 5.8 GHz

Fig. 10. Confusion matrices for the first two FC-DNN models, designed for drone detection and drone type identification. See Table 3 for the class labeling.

The obtained result of 98.6% for the average accuracy of the drone detection in 2.4 GHz ISM band is marginally worse compared to the work in (Al-Sa'd et al., 2019) where the achieved result was 99.7%. The main reason for this occurrence lies in the fact that a more representative RF background (ambient noise) was used in this research (simulated Bluetooth and Wi-Fi signals during the first step of each experiment that were used). Furthermore, in the process of dividing the whole considered RF signal into snapshots of data consisting of 100.000 samples (RF signal segmentation), the segments that do not contain a useful signal were not discarded. However, the obtained result of 99.8% for the average accuracy of drone detection in 5.8 GHz ISM band is better compared to the work in (Al-Sa'd et al., 2019). This is an expected result because the 5.8 GHz ISM band tends to be less crowded than the 2.4 GHz ISM band since fewer devices use it and because it has more allocated channels.

The average accuracy of the drone number detection is very high in

both ISM bands. This phenomenon can be explained with the following evidence: spectrograms for RF background and RF drone radio communications are quite dissimilar, and it is easy to visually distinguish different RF activities in spectrogram when two or three drones operate simultaneously. This result is an outstanding outcome of this research, and more importantly, it is independent of the ISM bands that are observed. The obtained results for the average accuracy of the drone number detection of 96.2% and 97.3% in 2.4 and 5.8 GHz ISM bands, respectively, are better compared with the work in (W. Zhang & Li, 2018) where the achieved result was 94.2% but for the radar sensor. Also, these results are an excellent basis for possible research on the application of DL algorithms in the detection of drone swarming.

Detection of the drone's type is considerably improved in comparison to similar studies. This resulted from the fact that the signal pre-processing step is enhanced by using power spectrum calculation (spectral energy distribution), instead of a discrete Fourier transform

Predicted Class	1	2	3	4	5	6	7	8	9	10	11	12	13	Target Class
1	84.2% 15.8%	96.2% 3.8%	72.2% 27.8%	77.5% 22.5%	80.9% 19.1%	73.5% 26.5%	81.8% 18.2%	88.0% 12.0%	94.4% 5.6%	88.3% 11.7%	87.5% 12.5%	81.8% 18.2%	83.4% 16.6%	88.5% 11.5%
2	96.2% 72.2%	0 0.0%	19 4.4%	15 0.1%	29 0.3%	75 0.7%	0 0.0%	0 0.0%	0 0.0%	0 0.0%	0 0.0%	0 0.0%	1 0.0%	92.7% 7.3%
3	72.2% 27.8%	0 0.0%	447 0.3%	15 5.1%	29 0.5%	50 0.4%	45 0.0%	1 0.0%	2 0.0%	3 0.0%	0 0.0%	0 0.0%	1 0.0%	78.8% 21.2%
4	77.5% 22.5%	0 0.0%	34 0.3%	512 5.1%	50 0.5%	45 0.4%	1 0.0%	1 0.0%	2 0.0%	3 0.0%	0 0.0%	0 0.0%	1 0.0%	78.6% 21.4%
5	80.9% 19.1%	0 0.0%	24 0.2%	57 0.6%	532 5.3%	30 0.3%	1 0.0%	0 0.0%	1 0.0%	0 0.0%	0 0.0%	0 0.0%	1 0.0%	82.4% 17.6%
6	73.5% 26.5%	1 0.1%	106 0.3%	30 4.9%	26 0.3%	488 0.0%	2 0.0%	0 0.0%	0 0.0%	0 0.0%	1 0.0%	1 0.0%	3 0.0%	74.2% 25.8%
7	81.8% 18.2%	0 0.0%	29 0.3%	17 0.2%	13 0.1%	9 6.0%	599 0.3%	29 0.2%	18 0.3%	35 0.1%	13 0.1%	9 0.1%	15 0.1%	75.4% 24.6%
8	88.0% 12.0%	0 0.0%	0 0.0%	0 0.0%	0 0.0%	1 0.2%	17 5.8%	579 0.0%	3 0.1%	15 0.1%	6 0.1%	10 0.1%	9 0.1%	89.6% 10.4%
9	94.4% 5.6%	0 0.0%	0 0.0%	3 0.0%	2 0.0%	0 0.0%	2 0.0%	613 6.1%	5 0.0%	0 0.0%	1 0.0%	0 0.0%	1 0.0%	97.5% 2.5%
10	88.3% 11.7%	0 0.0%	0 0.0%	0 0.0%	0 0.0%	0 0.0%	10 0.1%	7 0.1%	571 0.1%	7 0.0%	4 0.0%	7 0.0%	4 0.0%	91.7% 8.3%
11	87.5% 12.5%	0 0.0%	0 0.0%	0 0.0%	1 0.0%	1 0.0%	4 0.0%	15 0.1%	0 0.0%	9 0.0%	578 0.0%	16 0.2%	18 0.2%	88.8% 11.2%
12	81.8% 18.2%	0 0.0%	11 0.1%	20 0.2%	9 0.1%	3 0.0%	6 0.1%	8 0.1%	9 0.1%	13 0.1%	20 0.2%	559 0.2%	19 0.2%	79.3% 19.7%
13	83.4% 16.6%	0 0.0%	0 0.0%	3 0.0%	0 0.0%	5 0.0%	10 0.1%	15 0.1%	4 0.0%	7 0.0%	15 0.1%	32 0.3%	564 0.3%	82.6% 17.4%
	100.0% 0.0%	66.7% 33.3%	76.4% 23.6%	79.4% 20.6%	72.8% 27.2%	89.4% 10.6%	86.4% 13.6%	91.5% 8.5%	85.2% 14.8%	86.3% 13.7%	83.4% 16.6%	84.2% 15.8%	86.4% 13.6%	85.9% 14.1%

(a) drone type and flight (operational) mode identification with 13 classes in 2.4 GHz

Predicted Class	1	2	3	4	5	6	7	8	9	10	11	12	13	Target Class	
1	85.3% 14.7%	98.6% 1.4%	78.2% 21.8%	84.9% 15.1%	84.4% 15.6%	84.6% 15.4%	73.0% 27.0%	82.7% 17.3%	87.5% 12.5%	91.2% 8.8%	80.4% 19.6%	85.9% 14.1%	86.1% 13.9%	90.9% 9.1%	
2	98.6% 1.4%	2010 20.0%	1 0.0%	1 0.0%	3 0.0%	0 0.0%	0 0.0%	1 0.0%	1 0.0%	35 0.0%	4 0.0%	1 0.0%	6 0.0%	4 0.0%	97.2% 2.8%
3	78.2% 21.8%	0 0.0%	533 5.3%	53 0.5%	23 0.2%	32 0.3%	8 0.1%	11 0.1%	6 0.1%	1 0.0%	6 0.1%	7 0.1%	8 0.1%	5 0.0%	76.9% 23.1%
4	84.9% 15.1%	0 0.0%	43 0.4%	555 5.5%	18 0.2%	12 0.1%	1 0.0%	1 0.0%	0 0.0%	1 0.0%	2 0.0%	2 0.0%	1 0.0%	1 0.0%	87.1% 12.9%
5	84.4% 15.6%	0 0.0%	16 0.2%	15 0.1%	550 5.5%	34 0.3%	2 0.0%	1 0.0%	6 0.1%	1 0.0%	1 0.0%	3 0.0%	5 0.0%	86.8% 13.2%	
6	84.6% 15.4%	0 0.0%	14 0.1%	8 0.2%	20 0.2%	535 5.3%	3 0.0%	3 0.0%	2 0.0%	0 0.0%	2 0.0%	6 0.1%	1 0.0%	1 0.0%	89.9% 10.1%
7	73.0% 27.0%	0 0.0%	45 0.4%	36 0.3%	29 0.3%	34 0.3%	588 5.9%	70 0.7%	33 0.3%	27 0.3%	33 0.3%	36 0.3%	12 0.1%	12 0.1%	62.4% 37.6%
8	82.7% 17.3%	0 0.0%	4 0.0%	1 0.0%	5 0.0%	46 0.0%	555 0.5%	30 0.5%	12 0.3%	11 0.1%	0 0.0%	2 0.0%	1 0.0%	1 0.0%	82.6% 17.4%
9	87.5% 12.5%	0 0.0%	2 0.0%	3 0.0%	9 0.1%	10 0.1%	12 0.2%	17 0.2%	579 5.8%	14 0.1%	1 0.0%	2 0.0%	3 0.0%	1 0.0%	88.7% 11.3%
10	91.2% 8.8%	0 0.0%	0 0.0%	1 0.0%	1 0.0%	1 0.0%	7 0.1%	4 0.1%	4 0.0%	576 5.7%	0 0.0%	0 0.0%	0 0.0%	0 0.0%	97.0% 3.0%
11	80.4% 19.6%	0 0.0%	3 0.0%	0 0.0%	2 0.0%	1 0.0%	3 0.0%	2 0.0%	1 0.0%	487 4.8%	12 0.1%	13 0.1%	17 0.2%	17 0.1%	89.9% 10.1%
12	85.9% 14.1%	0 0.0%	4 0.0%	2 0.0%	7 0.1%	4 0.0%	1 0.0%	6 0.1%	1 0.0%	557 0.2%	13 0.1%	11 0.1%	11 0.1%	11 0.1%	90.9% 11.0%
13	86.1% 13.9%	0 0.0%	2 0.0%	1 0.0%	1 0.0%	2 0.0%	1 0.0%	0 0.0%	1 0.0%	81 0.8%	32 0.3%	604 0.6%	7 0.1%	82.4% 17.6%	
	100.0% 0.0%	79.6% 20.4%	82.8% 17.2%	82.1% 17.9%	79.9% 20.1%	87.8% 12.2%	82.8% 17.3%	86.4% 13.6%	86.0% 14.0%	72.7% 13.6%	83.1% 16.5%	90.1% 9.9%	90.3% 9.7%	86.9% 13.1%	

(b) drone type and flight (operational) mode identification with 13 classes in 5.8 GHz

Fig. 11. Confusion matrices for the third FC-DNN model, designed for the drone's flight mode identification. See Table 3 for the class labeling.

(DFT) of the signal. Such improvement was implemented with a modified built-in MatLab function (pspectrum) that finds a compromise between the spectral resolution achievable with the entire length of the signal and the performance limitations that result from computing large FFT. Moreover, the usage of improved FC-DNN models (deeper network with a combination of different activation functions) has also contributed to the improvement of the obtained results. Accordingly, the achieved results for the average accuracy of the drone's type identification of 96.1% and 95.7% in 2.4 and 5.8 GHz ISM bands, respectively, are significantly better compared to the work in (Al-Sa'd et al., 2019) where the achieved result was 84.5%.

Identification of the flight modes is the least accurate. This can be

attributed to the fact that spectrograms for different flight modes from one drone can be very similar. The obtained results for the average accuracy of the drone's flight mode identification of 85.9% and 86.9% in 2.4 and 5.8 GHz ISM bands, respectively, are better compared to the work in (Al-Sa'd et al., 2019) where the achieved result was 46.8%. Moreover, these particular results are not so essential, because in a real-world ADRO system it will not be necessary to detect all flight modes, but perhaps just hovering and flying with video recording.

There is an evident deterioration in the performance of FC-DNN when increasing the number of classes. This phenomenon can be explained by the similarities of RF drone communications, which are in this case all from the same manufacturer. This can be observed by examining the similarities in spectrograms presented in the supplementary material. The aforementioned introduces a challenging obstacle that can be mitigated using deeper neural networks or by other advanced classification algorithms. This is demonstrated in this research because authors in (Al-Sa'd et al., 2019) just used three hidden layers with ReLU activation function, as opposed to the six hidden layers with a combination of activation functions introduced in this algorithm.

The proposed algorithm achieved better results compared to other state-of-the-art algorithms. The proposed algorithm achieved accuracy that is in a class of prominent DL algorithms, and achieved stable results in both ISM bands, with a margin which is less than  $\pm 2\%$ . Furthermore, we can point out that the AlexNet (representative of CNN), the LSTM (representative of recurrent neural networks), and the proposed algorithm achieved exceptional results. The slightly worse results achieved by CNN algorithms can be explained by the fact that some useful information can be loose due to the preparing images for DNN input because of size-reducing operation.

It is noticeable that these results are slightly better than the results in (Al-Sa'd et al., 2019), which testify that new records in the introduced and publicly available RF drone dataset (Sazdić-Jotić et al., 2020) have verified for further use. The implementation of a developed drone RF dataset demonstrates the feasibility of confident drone detection and identification system.

## 5. Conclusion and future works

The contribution of this article is creating a new RF drone dataset consisting of records from the three experiments (one experiment with individually operating drones and two experiments with two and three drones operating simultaneously). Such dataset will be a preliminary point for a practical anti-drone system because it includes the RF signals of different drone types in different flight modes, so it can be used for testing and validation of the advanced, intelligent algorithms and can be adopted for researching and developing anti-drone systems with possibilities of detecting and identifying drones, and their current flight mode. Furthermore, FC-DNN models were tested, verified, and proved that this RF drone dataset can be used for developing new, possibly more effective DL algorithms in the future. Experimental results showed that the proposed algorithm in an indoor environment can detect a single drone with the probability of 99.8%, and identify drones with the probability of 96.1%. The proposed algorithm provides better results than other state-of-the-art algorithms. Additionally, it was demonstrated that multiple drones detection is possible with the proposed algorithm with high accuracy of 97.3%, which is according to the best of our knowledge a very significant outcome. Extending this RF drone dataset and fusing it with other drone detection approaches, such as optoelectronic images and videos, radar echoes, and acoustic recordings can improve the performance of the detection and identification system by exploiting the strengths of each modality. Furthermore, it is possible to explore the effect of different activation functions' combinations together with deeper neural network structure on the performance of the proposed FC-DNN models. The proposed methodology used in this paper performed very well during the testing phase, which was conducted within this research, and the results suggest that it has a potential for

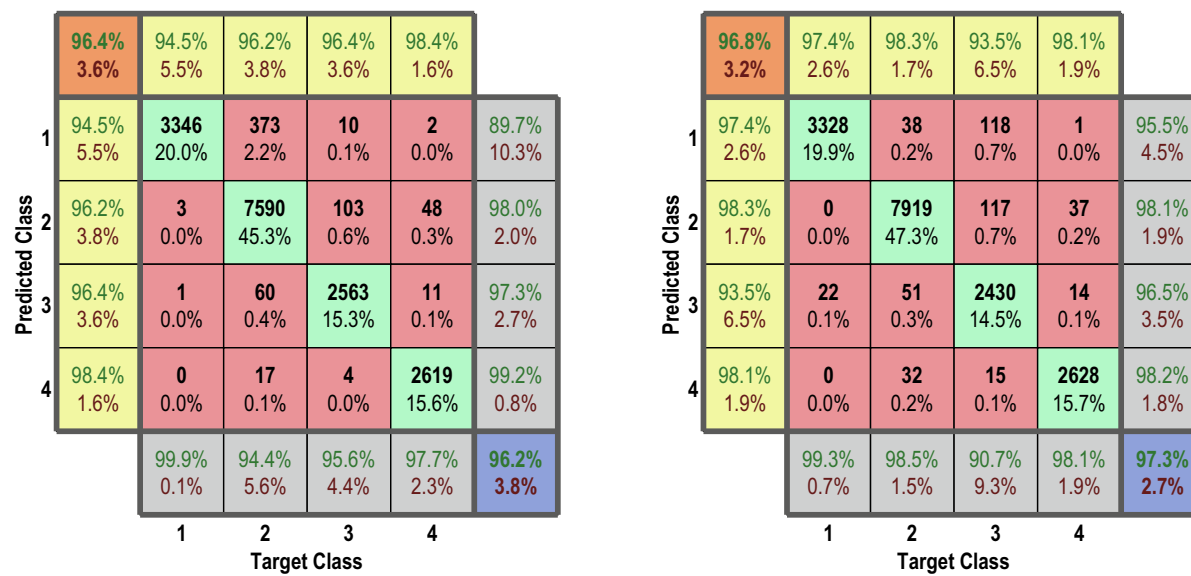


Fig. 12. Average classification performance for the fourth designed FC-DNN model using confusion matrices. See Table 3 for the class labeling.

Table 5  
Comparison of obtained average accuracy with the state-of-the-art ML and DL algorithms.

ALGORITHM	DETECTION ACCURACY				TYPE IDENTIFICATION ACCURACY				FLIGHT MODE IDENTIFICATION ACCURACY				MULTIPLE DRONES NUMBER DETECTION ACCURACY			
	Literature		Our dataset		Literature		Our dataset		Literature		Our dataset		Literature		Our dataset	
			2.4 GHz	5.8 GHz			2.4 GHz	5.8 GHz			2.4 GHz	5.8 GHz			2.4 GHz	5.8 GHz
AlexNet	–	97.1	90.0	–	94.4	85.3	–	86.0	80.3	–	97.4	71.0				
ResNet-18	–	96.8	92.9	–	95.9	85.8	–	90.7	80.1	–	97.3	87.0				
SqueezeNet	–	96.6	83.4	–	93.1	82.4	–	87.2	78.2	–	97.1	76.4				
LSTM SJB	–	96.2	99.5	–	92.2	94.2	–	85.4	84.8	–	93.2	90.8				
(Al-Emadi & Al-Senaidi, 2020)	99.8	96.0	99.7	85.8	93.5	96.7	59.2	81.4	73.3	–	96.0	97.1				
(Parlin et al., 2020)	97.3	96.3	–	–	–	–	–	–	–	–	–	–				
(Ezuma et al., 2020) k-Nearest Neighbor (kNN)	–	95.1	94.1	98.1	83.3	75.2	–	70.1	62.9	–	85.5	79.5				
(Ezuma et al., 2020) Support Vector Machine	–	94.9	87.1	96.5	59.5	58.4	–	48.5	42.7	–	72.6	69.2				
Proposed approach based on (Al-Sa'd et al., 2019)	99.7	98.6	99.8	84.5	96.1	95.7	46.8	85.9	86.9	–	96.2	97.3				

practical implementation in real case scenarios. This research can be extended in various ways such as: expanding the existing dataset by conducting experiments for indoor and outdoor conditions with various sensors (RF, audio, OES, and radar), using other types of drones where drones speed vary and distance from the RF sensors has greatened, the effects on FC-DNN accuracy can be examined by taking into consideration channel fading, noise or jamming signals, and by performing different spectrum calculations. The research and development of algorithms that include multimodal fusion will be the main objective in future work. The intention is to connect the proposed FC-DNN algorithm with the LSTM algorithm to exploit data from RF and audio sensors. Moreover, the multimodal fusion implementation in the GPU environment and testing in real situations will be the ultimate ADRO research goal.

#### CRediT authorship contribution statement

**Boban Sazdić-Jotić:** Conceptualization, Data curation, Software, Writing - original draft. **Ivan Pokrajac:** Supervision, Investigation, Validation. **Jovan Bajčetić:** Visualization, Investigation, Writing -

review & editing. **Boban Bondžulić:** Methodology, Supervision, Writing - review & editing. **Danilo Obradović:** Data curation, Writing - review & editing.

#### Declaration of Competing Interest

The authors declare that they have no known competing financial interests or personal relationships that could have appeared to influence the work reported in this paper.

#### Acknowledgments

This research is conducted under the project funded by the University of Defence in Belgrade Grant No. VA-TT/3/20-22 and the project RABAMADRIDS funded by the Military Technical Institute (MTI) in Belgrade. The findings achieved herein are solely the responsibility of the authors.

## Appendix A. Supplementary data

Supplementary data to this article can be found online at <https://doi.org/10.1016/j.eswa.2021.115928>.

## References

- Abeywickrama, S., Jayasinghe, L., Fu, H., Nissanka, S., & Yuen, C. (2018). RF-based Direction Finding of UAVs Using DNN. 2018 IEEE International Conference on Communication Systems (ICCS), 157–161. 10.1109/ICCS.2018.8689177.
- Al-Emadi, S., & Al-Senaid, F. (2020). Drone detection approach based on radio-frequency using convolutional neural network. In 2020 IEEE International Conference on Informatics, IoT, and Enabling Technologies (ICIoT). <https://doi.org/10.1109/ICIoT48696.2020.9089489>
- Al-Sa'd, M. F., Al-Ali, A., Mohamed, A., Khattab, T., & Erbad, A. (2019). RF-based drone detection and identification using deep learning approaches: an initiative towards a large open source drone database. *Future Generation Computer Systems*, 100, 86–97. <https://doi.org/10.1016/j.future.2019.05.007>
- Alhadrami, E., Al-Mufti, M., Taha, B., & Werghi, N. (2019). Learned micro-Doppler representations for targets classification based on spectrogram images. *IEEE Access*, 7, 139377–139387. <https://doi.org/10.1109/ACCESS.2019.2943567>
- Basak, S., Rajendran, S., Pollin, S., & Scheers, B. (2021). Drone classification from RF fingerprints using deep residual nets. 2021 International Conference on COMmunication Systems & NETworkS (COMSNETS), 548–555. 10.1109/COMSNETSS51098.2021.9352891.
- D-Fend. (2021). D-Fend Solutions A.D. Ltd. <https://www.d-fendsolutions.com/>.
- DJI. (2021). DJI. <https://www.dji.com/>.
- Erzuma, M., Erden, F., Kumar Anjinappa, C., Ozdemir, O., & Guvenc, I. (2020). Detection and classification of UAVs using RF fingerprints in the presence of Wi-Fi and bluetooth interference. *IEEE Open Journal of the Communications Society*, 1, 60–76. <https://doi.org/10.1109/OJCOMS1.1109.0JCOMS.2019.2955889>
- Hassanalian, M., & Abdelkefi, A. (2017). Classifications, applications, and design challenges of drones: A review. *Progress in Aerospace Sciences*, 91(2017), 99–131. <https://doi.org/10.1016/j.paerosci.2017.04.003>
- Karita, S., Watanabe, S., Iwata, T., Ogawa, A., & Delcroix, M. (2018). Semi-Supervised End-to-End Speech Recognition. Interspeech 2018, 2–6. 10.21437/Interspeech.2018-1746.
- Kim, Y. (2014). Convolutional neural networks for sentence classification. In *Proceedings of the 2014 Conference on empirical methods in natural language processing (EMNLP)* (pp. 1746–1751). <https://doi.org/10.3115/v1/D14-1181>
- Krizhevsky, A., Sutskever, I., & Hinton, G. E. (2017). ImageNet classification with deep convolutional neural networks. *Communications of the ACM*, 60(6), 84–90. <https://doi.org/10.1145/3065386>
- Manessi, F., & Rozza, A. (2018). Learning Combinations of Activation Functions. Proceedings – International Conference on Pattern Recognition, 2018-Augus, 61–66. 10.1109/ICPR.2018.8545362.
- MathWorks. (2021). Deep learning for signal processing with MATLAB. <https://www.mathworks.com/campaigns/offers/deep-learning-for-signal-processing-white-paper.html?elqCampaignId=10588>.
- Mitka, E., & Mouroutsos, S. G. (2017). Classification of drones. *American Journal of Engineering Research (AJER)*, 6(7), 36–41. [http://www.ajer.org/papers/v6\(07\)/F06073641.pdf](http://www.ajer.org/papers/v6(07)/F06073641.pdf).
- Nair, V., & Hinton, G. E. (2009). 3D object recognition with deep belief nets. Advances in Neural Information Processing Systems 22 - Proceedings of the 2009 Conference, 22, 1339–1347. <https://proceedings.neurips.cc/paper/2009/file/6e7b33fdea3adc80ebd648ffb665bb8-Paper.pdf>.
- Narkhede, P., Walambe, R., Mandaokar, S., Chandel, P., Kotecha, K., & Ghinea, G. (2021). Gas detection and identification using multimodal artificial intelligence based sensor fusion. *Applied System Innovation*, 4(1), 1–14. <https://doi.org/10.3390/asi4010003>
- Nguyen, P., Ravindranath, M., Nguyen, A., Han, R., & Vu, T. (2016). Investigating cost-effective RF-based detection of drones. Proceedings of the 2nd Workshop on Micro Aerial Vehicle Networks, Systems, and Applications for Civilian Use, October 2018, 17–22. 10.1145/2935620.2935632.
- Nick Winovich. (2021). Deep Learning. [https://www.math.purdue.edu/~nwinovic/deep\\_learning.html](https://www.math.purdue.edu/~nwinovic/deep_learning.html).
- Parlin, K., Riihonen, T., Karm, G., & Turunen, M. (2020). Jamming and classification of drones using full-duplex radios and deep learning. IEEE International Symposium on Personal, Indoor and Mobile Radio Communications, PIMRC, 2020-Augus. 10.1109/PIMRC48278.2020.9217351.
- Patel, J., Shah, S., Thakkar, P., & Kotecha, K. (2015). Predicting stock and stock price index movement using Trend Deterministic Data Preparation and machine learning techniques. *Expert Systems with Applications*, 42(1), 259–268. <https://doi.org/10.1016/j.eswa.2014.07.040>
- Pathak, A. R., Pandey, M., & Rautaray, S. (2018). Application of deep learning for object detection. *Procedia Computer Science*, 132, 1706–1717. <https://doi.org/10.1016/j.procs.2018.05.144>
- Peacock, M., & Johnstone, M. N. (2013). Towards detection and control of civilian Unmanned Aerial Vehicles. Australian Information Warfare and Security Conference, June, 1–8. 10.4225/75/57a847dfbefb5.
- Peng, S., Jiang, H., Wang, H., Alwageed, H., Zhou, Y., Sebdani, M. M., & Yao, Y.-D. (2019). Modulation classification based on signal constellation diagrams and Deep Learning. *IEEE Transactions on Neural Networks and Learning Systems*, 30(3), 718–727. <https://doi.org/10.1109/TNNLS.2018.2850703>
- Sazdić-Jotić, B. M., Pokrajac, I., Bajčetić, J., Bondžulić, B. P., Joksimović, V., Šević, T., & Obradović, D. (2020). VTL\_DroneSET\_FFT. Mendelej Data. 10.17632/s6tgnnp5n2.1.
- Šević, T., Joksimović, V., Pokrajac, I., Radana, B., Sazdić-Jotić, B., & Obradović, D. (2020). Interception and detection of drones used by RF-based dataset of drones. *Scientific Technical Review*, 70(2), 29–34.
- Yaacoub, J.-P., Noura, H., Salman, O., & Chehab, A. (2020). Security analysis of drones systems: Attacks, limitations, and recommendations. *Internet of Things*, 11(100218), Article 100218. <https://doi.org/10.1016/j.iot.2020.100218>
- Zha, X., Peng, H., Qin, X., Li, G., & Yang, S. (2019). A Deep Learning framework for signal detection and modulation classification. *Sensors*, 19(18), 4042. <https://doi.org/10.3390/s19184042>
- Zhang, H., Cao, C., Xu, L., & Gulliver, T. A. (2018). A UAV detection algorithm based on an artificial neural network. *IEEE Access*, 6, 24720–24728. <https://doi.org/10.1109/ACCESS.2018.2831911>
- Zhang, W., & Li, G. (2018). Detection of multiple micro-drones via cadence velocity diagram analysis. *Electronics Letters*, 54(7), 441–443. <https://doi.org/10.1049/el.2017.4317>
- Zhong, H., Chen, Z., Qin, C., Huang, Z., Zheng, V. W., Xu, T., & Chen, E. (2020). Adam revisited: A weighted past gradients perspective. *Frontiers of Computer Science*, 14(5), Article 145309. <https://doi.org/10.1007/s11704-019-8457-x>
- Zhou, S., Yin, Z., Wu, Z., Chen, Y., Zhao, N., & Yang, Z. (2019). A robust modulation classification method using convolutional neural networks. *EURASIP Journal on Advances in Signal Processing*, 2019(1), 21. <https://doi.org/10.1186/s13634-019-0616-6>